Supporting Information

A One-Step Immunoassay of Tau Protein Based on Flow Cytometric Counting of Target-Induced Nanoaggregates

Junyue Sun,†[a] Yan Qi,†[b] Jing Zhang,*[a] Wei Ren*[a] and Chenghui Liu[a]

* Corresponding authors

[a] Key Laboratory of Applied Surface and Colloid Chemistry, Ministry of Education; Key Laboratory of Analytical Chemistry for Life Science of Shaanxi Province; School of Chemistry & Chemical Engineering, Shaanxi Normal University, Xi'an 710119 Shaanxi Province, P. R. China

Email: zhangjing8902@snnu.edu.cn, wei.ren@snnu.edu.cn

[b] Institute of Basic and Translational Medicine & Shaanxi Key Laboratory of Brain Disorders and Engineering Research Center of Brain Diseases Drug Development, Universities of Shaanxi Province, Xi'an Medical University, Xi'an 710021 Shaanxi Province, P. R. China

† These authors contributed equally to this work.

List of Contents：

1. Materials and reagents

Streptavidin (STV)-coated magnetic nanobeads (~300 nm) were purchased from Ademtech (Pessac, France). Tau protein was purchased from Abcam (Waltham, MA, USA). Biotinylated Tau monoclonal tau-12 antibody (tau Ab1) was purchased from Biolegend (San Diego, CA, USA). Biotinylated monoclonal tau HT7 antibody (tau Ab2) was purchased from Thermo Fisher Scientific (Waltham, MA, USA). Amyloid β-protein (Aβ) was purchased from Shanghai Chairbio Technology Co., Ltd (Shanghai, China). Prostate-specific antigen (PSA), cardiac troponin I (cTnI), and corresponding biotinylated antibody pairs, including monoclonal capture antibody (Ab1) and monoclonal detection antibody (Ab2) were purchased from Shanghai Linc-Bio Science Co., Ltd (Shanghai, China). Alpha-fetoprotein (AFP) and carcinoembryonic antigen (CEA) were purchased from Shanghai Linc-Bio Science Co., Ltd (Shanghai, China). Bovine serum albumin (BSA) was purchased from Sigma-Aldrich (St. Louis, MO, USA). 20 × SSC buffer (3 M NaCl, 300 mM sodium citrate, pH = 7) and Tween-20 were obtained from Sangon Biotech (Shanghai, China). Fetal bovine serum (FBS) was purchased from Procell Life Science & Technology Co., Ltd (Wuhan, China). The AlexaFluor488 (AF488)/biotin-labeled and Cyanine 5 (Cy5)/biotin-labeled two fluorescence probes were synthesized by Sangon Biotech (Shanghai, China), and the detailed sequences are listed in Table S1.

Table S1. The DNA sequences used in this study

Name	Sequence (5'-3')
AF488 fluorophore-labelled probe	biotin- $(T)_{10}$- Alexa Flour 488
Cy5 fluorophore-labelled probe	biotin- $(T)_{10}$- Cyanine 5

2. Detailed experimental procedures

Functionalization of the nanobeads

Firstly, 0.07 mg nanobeads (~1.2×10^{10}) were pipetted out and dispersed in a 1 × SSCT-BSA buffer (150 mM NaCl, 15 mM sodium citrate, 0.1% v/v Tween-20, 5% w/v BSA, pH = 7.0). Then, 8.4 μg biotinylated antibody Tau Ab1 and 140 pmol of biotin/Alexa Flour 488 (AF488) fluorophore-labelled probe were added to the solution and incubated for 0.5 h at room temperature. Thereby, both the fluorescent probes and the Tau Ab1 antibodies were immobilized on the nanobeads through the STV-biotin interaction, producing Ab1-AF488-nanobeads. Additionally, another 0.07 mg Ab2-Cy5-nanobeads co-immobilized with the biotinylated antibody Tau Ab2 and Cyanine 5 (Cy5) fluorophore-labelled probe were prepared according to the same procedures. After magnetic purification, the two types of nanobeads were respectively resuspended in 45 mL 1 × SSCT-BSA buffer and stored at 4 °C for future use.

Standard procedure of tau protein detection based on target-induced aggregation

The functionalized nanobeads and Tau protein were diluted by 1 × SSCT-BSA to the required concentrations. Simply, the two types of the above prepared nanobeads (~2.4×10^6, respectively) and a series concentrations of Tau protein were added to conduct the sandwich immunoreaction between two nanobeads in 10 μL of 1 × SSCT-BSA buffer for 1.5 h at room temperature under shaking. The 10 μL reaction system comprised: 1 μL Ab1-488-nanobeads (~2.4×10^6 beads/μL), 1 μL Ab2-Cy5-nanobeads (~2.4×10^6 beads/μL), 1 μL Tau protein solution at varying concentrations, and 7 μL 1 × SSCT-BSA. And then, the reaction mixture was diluted to 300 μL with 1 × SSC buffer and analyzed with a flow cytometer (BD Biosciences, BD FACSCelesta). For each sample, 10,000 events were monitored one-by-one at the FL1 (AF488) and FL4 (Cy5) channels under 488 nm and 640 nm excitation, respectively. In this way, the nanobeads of single-color and dual-color can be clearly discriminated. And the quantification of the protein target in each sample was achieved by evaluating the aggregation percentage of the detected nanobeads.

Optimization of nanobead number used in the proposed assay

The number of nanobeads can obviously influence the random collision probability between

two types of nanobeads. Thus, the number of each kind of nanobead used in the proposed assay was optimized from 1.2×10^5 to 4.8×10^6. As shown in Fig. S1, the aggregate percentage produced by blank control increases slowly and then remains stable as the number of nanobeads increases from 1.2×10^5 to 4.8×10^6. Meanwhile, as the number of nanobeads increased from 1.2×10^5 to 2.4×10^6, the aggregate percentages gradually increased. However, the aggregate percentages will be decreased when the number of nanobeads continues to increase to 4.8×10^6. Therefore, 2.4×10^6 of each nanobead was chosen as the optimum in this assay.

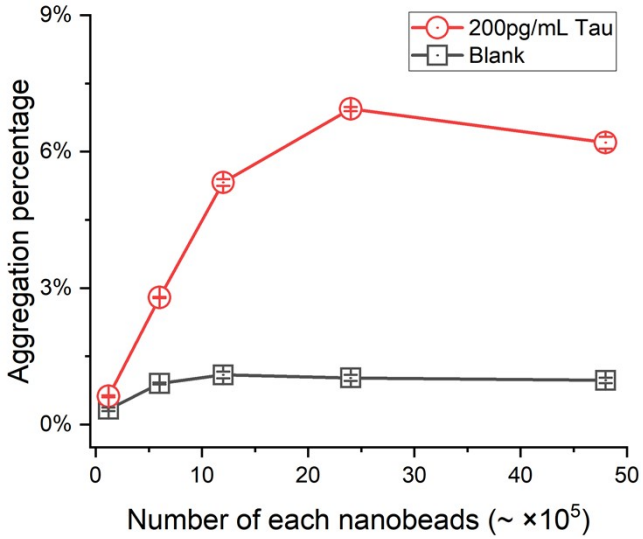

Fig. S1. Evaluation of the number of nanobeads used in the proposed assay. The Tau protein concentration was fixed at 200 pg/mL.

3. Generality of the proposed flow cytometric immunoassay

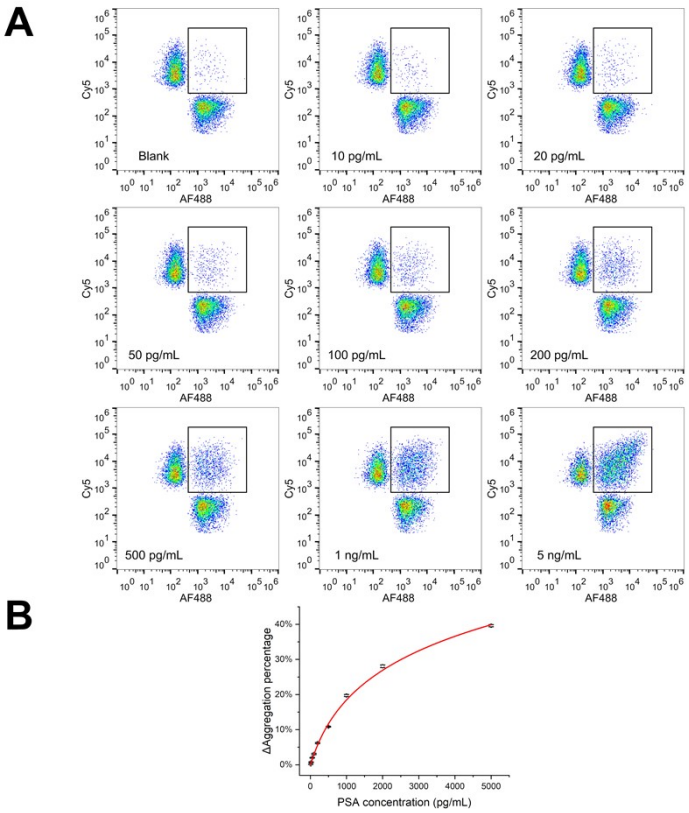

Fig. S2. (A) The AF488 *vs.* Cy5 scatter plots of the nanobeads in the presence of different concentrations of PSA. (B) The relationship between the aggregation percentage and the concentration of PSA. Error bars represent the standard deviation of 3 replicate tests.

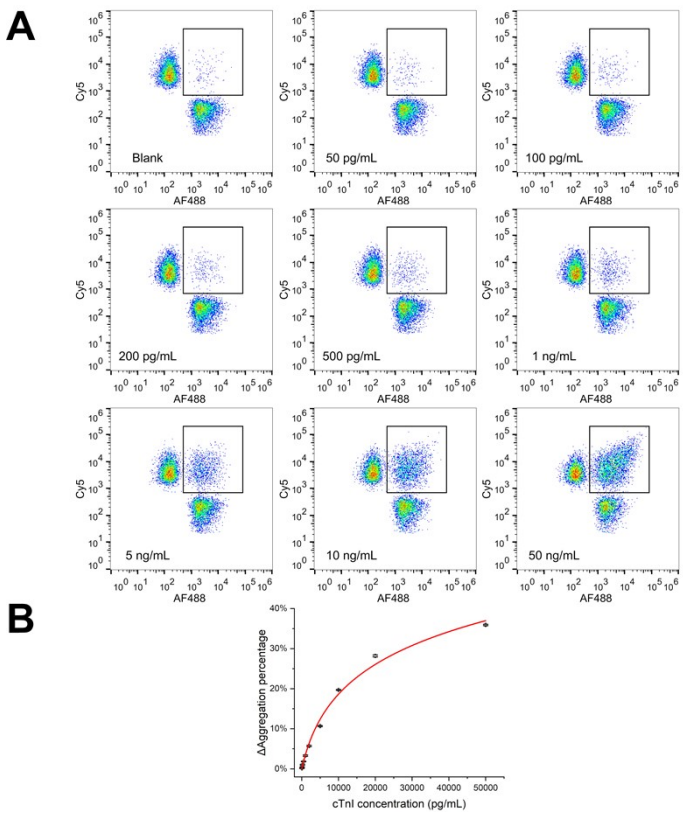

Fig. S3. (A) The AF488 *vs.* Cy5 scatter plots of the nanobeads in the presence of different concentrations of cTnI. (B) The relationship between the aggregation percentage and the concentration of cTnI. Error bars represent the standard deviation of 3 replicate tests.

The versatility of the nanobead-aggregation assay strategy is investigated by detecting prostate-specific antigen (PSA) and cardiac troponin I (cTnI) (Fig. S2 and Fig. S3), respectively by using PSA- and cTnI-specific antibody pairs. Similar to the Tau protein results, the percentage of dual-color nanobead aggregates increases with the ascending concentration of PSA and cTnI, and both targets exhibit good logarithmic relationships between protein concentration and aggregate percentage. These results demonstrate that this strategy has good versatility for detecting different protein targets.

Specifically, as shown in Fig. S2B, there is a logarithmic relationship between PSA concentration (C_{PSA}, pg/mL) and aggregation percentage (P), the corresponding correlation equation is $\Delta P = 16.26 \ln (C_{PSA} + 464.85) - 100.10$ with $R^2 = 0.9963$.

As shown in Fig. S3B, there is a logarithmic relationship between cTnI concentration (C_{cTnI}, pg/mL) and aggregation percentage (P), the corresponding correlation equation is $\Delta P = 13.13 \ln (C_{cTnI} + 3167.38) - 105.94$ with $R^2 = 0.9953$.

4. Detection of Tau in biological sample

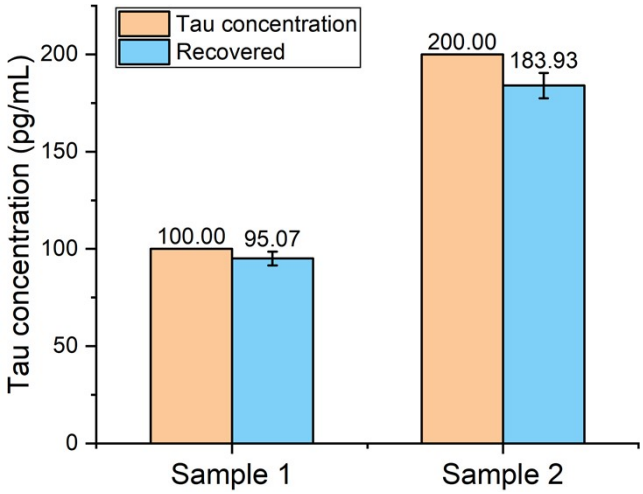

Fig. S4. The comparison of the added concentration (yellow) and actually detected concentration of Tau protein in FBS by the proposed strategy (blue).

To investigate the potential detection capability of this strategy in complex samples, it was evaluated by detecting the Tau protein spiked in fetal bovine serum (FBS). The 10 μL reaction system comprised: 1 μL Ab1-488-nanobeads (~2.4 × 10^6 beads/μL), 1 μL Ab2-Cy5-nanobeads (~2.4 × 10^6 beads/μL), 1 μL Tau protein solution, 6 μL 1 × SSCT-BSA and 1 μL 1% FBS (diluted by 1 × SSCT-BSA). The incubation conditions were identical to those described above. The recovery rates are calculated to be 95% and 92% when the concentrations of Tau protein were 100 pg/mL and 200 pg/mL, respectively (Fig. S4). All results indicate that this strategy has great potential in detecting proteins in complex samples.

5. Comparison of different bead-based immunoassays

Table S2. Comparison of different bead-based immunoassays

Sensing strategy	Bead Size	LOD/Lowest detectable concentration	Amplification Method	Number of Steps	Duration	Ref
Chemiluminescence imaging-based digital immunoassay	2.8 μm	50 fg/mL (PSA)	TSA-amplification	3	2.5 h	S1
FCM digital immunoassay	3.2 μm	7.22 fM (HE-4)	Rolling circle amplification	6	3 h	S2
Fluorescence imaging-based digital immunoassay	2.8 μm	0.022 pg/mL (Tau)	Rolling circle amplification	4	5 h	S3
FCM immunoassay	2.8 μm + 16 nm	0.5 pg/mL (PSA)	TdT-amplification	4	4 h	S4
Cellphone-enabled microbead aggregation assay	5 μm	0.125 ng/mL (PSA)	N/A	1	0.5 h	S5
Aggregation-collision-enabled electrochemical immunoassay	20 nm	5 pg/mL (AFP)	N/A	1	1 h	S6
Size-encoded the electrical resistance-based particle counting immunoassay	3 μm + 1 μm	0.12 ng/mL (Procalcitonin)	N/A	2	40 min	S7
Colorimetric and surface-enhanced Raman scattering dual-readout lateral flow assay	30-40 nm	1 pg/mL (Tau)	N/A	4	25 min	S8
AuNP aggregation enabled colorimetric immunoassay	150 nm	0.79 ng/mL (Enrofloxacin)	N/A	1	15 min	S9
FCM-based bead aggregation assay	2.8 μm	5 pg/mL (PSA)	N/A	1	1 h	S10
FCM-based bead aggregation assay	4 μm + 200 nm	22 pg/mL (PSA)	N/A	4	3 h	S11
FCM-based bead aggregation assay	300 nm	5 pg/mL (Tau)	N/A	1	1.5 h	This work

6. Comparison of different strategies for Tau detecting

Table S3. Comparison of different strategies for Tau detecting

Strategy	Capture antibody	Detection antibody	Antigen type	LOD/Lowest detectable concentration	Features	Ref.
Novel enzyme-linked immunosorbent assay	hTau441-E22A3	hTau p181-Rk27A6	p-tau181	3.06 pg/mL	Standard sandwich ELISA, resistant to contamination	S12
Microscopic imaging counting	Monoclonal Tau HT7	Monoclonal Tau12	Tau441	55.7 pg/mL	Tetraplex detection, amplification-free	S13
Dual-mode magnetic immunosensor	3G5	R1	p-tau (396,404)	SERS: 1.5 pg/mL Colorimetric: 24 pg/mL	Dual-signal readout, whole blood detection	S14
Semiconductor SERS platform	TauJ.5H3	N/A (Aptamer employed)	BD-Tau	0.028 pM	Enhanced Raman signals, visual diagnostic report	S15
Surface plasmon resonance imaging	R-anti-pT181	N/A	p-tau181	1.12 pg/mL	Label-free, 2D arrays/microarrays	S16
Light-initiated chemiluminescence assay	clone AT270	clone Tau12	p-tau181	0.19 pg/mL	Wash free, cost reduction, fully automated analysis	S17
Dual-readout lateral flow immunoassay	3G5	R1	p-tau (396,404)	SERS: 1 pg/mL Colorimetric: 40 pg/mL	Dual-signal readout, dual-target detection	S8
FCM-based bead aggregation assay	Monoclonal Tau12	Monoclonal Tau HT7	Tau441	5 pg/mL (0.11 pM)	One-step detection, simple protocol	This work

References

S1 C. Lei, Z. Tian, J. Shi, W. Fan, W. Ren, X. Duan and C. Liu, Sens. Actuators B Chem., 2026, **457**, 139710.

S2 S. J. Zhang, C. Wu and D. R. Walt, ACS Nano, 2024, **18**, 29891-29901.

S3 Y. Zhang, Y. An, M. Yang, Y. Huang, S. Yu, X. Xu and C. Yang, Sens. Actuators B Chem., 2026, **457**, 139727.

S4 L. Zhu, D. Chen, X. Lu, Y. Qi, P. He, C. Liu and Z. Li, Chem. Sci., 2018, **9**, 6605-6613.

S5 W. Cui, M. He, L. Mu, Z. Lin, Y. Wang, W. Pang, M. Reed and X. Duan, ACS Sens., 2018, **3**, 432-440.

S6 J.-H. Zhang, M. Liu, F. Zhou, H.-L. Yan and Y.-G. Zhou, Anal. Chem., 2023, **95**, 3045-3053.

S7 Z. Wang, J. Liu, Y. Yang, P. Li, K. Li, Y. Xianyu, Y. Chen and B. Li, Anal. Chem., 2021, **93**, 6178-6187.

S8 L. Zhang, X. Du, T. Zhang, Q. Chen, Q. Zhang, Y. Su, M. Zhang and H. Luo, Sens. Actuators B Chem., 2026, **451**, 139417.

S9 Y. Shen, F. Jia, A. Liang, Y. He, Y. Peng, H. Dai, Y. Fu, J. Wang and Y. Li, ACS Appl. Mater. Interfaces, 2022, **14**, 8816-8823.

S10 J. Sun, X. Fei, W. Fan, W. Ren, J. Zhang and C. Liu, Anal. Chem., 2025, **97**, 13514-13521.

S11 X. Min, S. Huang and C. Yuan, Anal. Chim. Acta, 2022, **1204**, 339704.

S12 T. Kawarabayashi, T. Nakamura, K. Miyashita, I. Fukamachi, Y. Seino and M. Shoji, Neurosci. Lett., 2020, **722**, 134826.

S13 X. Wu, R. Li, T. Lai, G. Tao, F. Liu and N. Li, Anal. Chem., 2021, **93**, 16873-16879.

S14 L. Zhang, K. Cao, Y. Su, S. Hu, X. Liang, Q. Luo and H. Luo, Biosens. Bioelectron., 2023, **222**, 114935.

S15 Y. Zhou, J. Li, T. Zheng and Y. Tian, Chem. Biomed. Imaging, 2023, **1**, 186-191.

S16 L. Oldak, Z. Zielinska, K. Socha, S. Bogdan and E. Gorodkiewicz, Talanta, 2024, **271**, 125736.

S17 Y. Yang and X. Wang, Analyst, 2025, **150**, 3838-3848.